J. Plasma Physics (1994), *vol.* 52, *part* 1, *pp.* 91–111

Copyright © 1994 Cambridge University Press

Tokamak divertor maps

By ALKESH PUNJABI, ARUN VERMA
Hampton University, Hampton, Virginia 23668, U.S.A.

AND ALLEN BOOZER
College of William and Mary, Williamsburg, Virginia 23185, U.S.A., and Max-Planck Institut fur Plasmaphysik, D8046 Garching, Germany

(Received 8 March 1994 and in revised form 8 May 1994)

A mapping method is developed to investigate the problem of determination and control of heat-deposition patterns on the plates of a tokamak divertor. The deposition pattern is largely determined by the magnetic field lines, which are mathematically equivalent to the trajectories of a single-degree-of-freedom time-dependent Hamiltonian system. Maps are natural tools to study the generic features of such systems. The general theory of maps is presented, and methods for incorporating various features of the magnetic field and particle motion in divertor tokamaks are given. Features of the magnetic field include the profile of the rotational transform, single- versus double-null divertor, reverse map, the effects of naturally occurring low M and N, and externally imposed high-M, high-N perturbations. Particle motion includes radial diffusion, pitch angle and energy scattering, and the electric sheath at the plate. The method is illustrated by calculating the stochastic broadening in a single-null divertor tokamak. Maps provide an efficient, economic and elegant method to study the problem of motion of plasma particles in the stochastic scrape-off layer.

1. Introduction

Divertors are a common feature of present-day large tokamaks. The heat fluxes striking the collector plates may be as high as 15–20 MW m^{-1}. Issues related to the heat flux deposition are of considerable importance for the design of future tokamaks. Therefore the prediction and preferably the control of the width of the scrape-off layer of a divertor is a central issue in the design of ignition tokamaks such as the international thermonuclear experimental reactor ITER (Post *et al.* 1991). Divertor simulations generally assume that the plasma is bounded by a sharp separatrix, which is correct only if the toroidal symmetry is perfect. Toroidal asymmetries in the magnetic field cause the toroidal magnetic flux inside the last confining magnetic surface to be smaller than the flux inside the unperturbed separatrix, and create a layer of open magnetic field lines that lies between the last confining magnetic surface and the unperturbed separatrix. This layer is called the stochastic layer. It is important to know the effects of naturally occurring perturbations, such as toroidal ripple or magnetohydrodynamic (MHD) modes, on the design of divertors. The introduction of magnetic perturbations may allow an optimization of the width of the divertor scrape-off layer and control of the heat deposition on the divertor plates. Thus the issue of heat deposition on divertor plates is of critical importance in tokamak physics.

We have developed a new approach to investigate this problem that makes use of what we call tokamak divertor maps. This approach is based on the observation that the magnetic field trajectories in a divertor tokamak are mathematically equivalent to a single-degree-of-freedom, time-dependent Hamiltonian system, and that the basic features of motion near a separatrix broadened by asymmetric perturbations are generic for such Hamiltonian and near-Hamiltonian systems. In this approach, the motion of field lines, including the effects of asymmetric perturbations, is represented by area-preserving maps and their continuous analogues, which we call tokamak divertor maps. The key results obtained using this method to calculate stochastic broadening in a single-null divertor were reported by Punjabi, Verma & Boozer (1992). In this paper we give a thorough exposition of the method, with a detailed discussion of how it is applied to the problem of determining the pattern of the strike points of particle trajectories on the divertor plates of a single-null divertor tokamak.

Pomphrey & Rieman (1992) have made related calculations using wires to model divertor configuration instead of a map. B. J. Braams & M. D. Teytel (1993 personal communication) have employed the grid-free random-walk method to study this problem. La Haye's (1991) work uses a differential-equation approach with a realistic magnetic geometry for the DIII-D device. Our mapping method, on the other hand, is much more computationally efficient and suitable for looking at detailed generic issues.

The remainder of this paper is organized in six sections. In §2 we state the purpose for developing this method, and describe the desirable features that we should like it to possess. In §3 we introduce the idea of Hamiltonian mechanics of a broadened separatrix. In §4 we introduce the simplest of the tokamak divertor maps, called the simple map. We also present some useful extensions of the simple map. These include a map for the double-null divertor tokamak, a continuous analogue of the simple map, the backward map, a map with high adjustable shear, and maps that include naturally occurring low poloidal and toroidal mode numbers (M and N) as well externally imposed high-M, high-N perturbations. We also give two methods for calculating the deposition pattern of field lines on the divertor plates. In §5 we give the general theory of maps, which forms the theoretical foundation for the tokamak divertor maps. In this section, we also discuss the generating functions for area-preserving maps, and the explicit, reversed and continuous maps. In §6 we discuss a Monte Carlo procedure for calculating the heat deposition on divertor plates. This procedure includes the effects of spatial diffusion, velocity-space scattering, energy scattering and the electric sheath at the divertor plate on the particle trajectories. In §7 we show in detail how the simple map is applied to a single-null divertor tokamak to calculate stochastic broadening of the scrape-off layer. We also summarize and discuss our results in this section.

2. Purpose of the method

Our purpose is to calculate the effects of magnetic asymmetries on the heat-deposition pattern on divertor plates, and to determine if the heat deposition can be broadened. We have developed a method called the method of maps to investigate this problem. This new method correctly addresses the issues of magnetic and particle effects. Magnetic effects involve the topology of the toroidal magnetic configuration, the width of the stochastic scrape-off layer, and the rotational-transform profiles. Particle effects include motion along the field lines, radial diffusion, and pitch angle and energy scattering. Since the mean free path of electrons in the stochastic scrape-off layer is comparable to the magnetic correlation length, a fluid treatment of this problem is not satisfactory. The method of maps is efficient, economical and flexible, and the physics of the method is transparent and clear.

In the simulations, which assume a sharp separatrix, the width of the scrape-off layer is determined by the assumed diffusion coefficient, which is usually of order 1 $m^2\,s^{-1}$. The field lines of the scrape-off layer strike the divertor plates in a stripe with a width that is determined by axisymmetric magnetics. For asymmetric perturbations the width of the stochastic layer near the X point is approximately proportional to the square root of the toroidally asymmetric perturbation amplitude (Boozer 1983). If the magnetic perturbations are sufficiently large, the scrape-off layer is dominated by the stochastic layer. The field lines of the stochastic layer strike the divertor plate in a stripe that is much narrower (by a factor of about six) than the stochastic region of magnetic flux that lies between the last confining magnetic surface and the ideal separatrix. One of the important quantities used in this paper is the width of the stochastic scrape-off layer. This width is measured as the distance from the X-point to the last confining magnetic surface, where the distance is measured along the line from the O-point to the X-point. The greater width of the scrape-off layer in comparison to the divertor stripe has important implications for the design of divertors.

3. Hamiltonian mechanics of a broadened separatrix

Any globally divergence-free field in 3-space is mathematically equivalent to a single-degree-of-freedom Hamiltonian system (Whittaker 1937; Cary & Littlejohn 1983; Lichtenberg & Liberman 1983). For example, the motion of magnetic field lines in a tokamak can be described in terms of a poloidal angle θ as the canonical co-ordinate, toroidal flux ψ as the canonical momentum, the negative of poloidal flux, namely $\chi = \chi(\psi, \theta, \phi)$, as the Hamiltonian, and a toroidal angle ϕ as the canonical time. The phase space of this Hamiltonian system can be extended by considering the negative of the Hamiltonian, namely $-\chi$, and ϕ as conjugate variables. The phase space is then three-dimensional, and phase flow is parametrized by canonical time. For closed magnetic confinement systems, invariant surfaces are nested tori in 3-space. These Hamiltonian systems have the same topological structure as the simple map. The basic features of the motion of these systems near a separatrix are generic. Therefore the Hamiltonian mechanics of the broadened separatrix is the natural approach to investigate the motion in the scrape-off layer of a divertor tokamak. This approach can be made efficient and economic if we can construct area-preserving discrete maps to represent the Hamiltonian systems. The continuous analogue of the maps should be solutions of the single-degree-

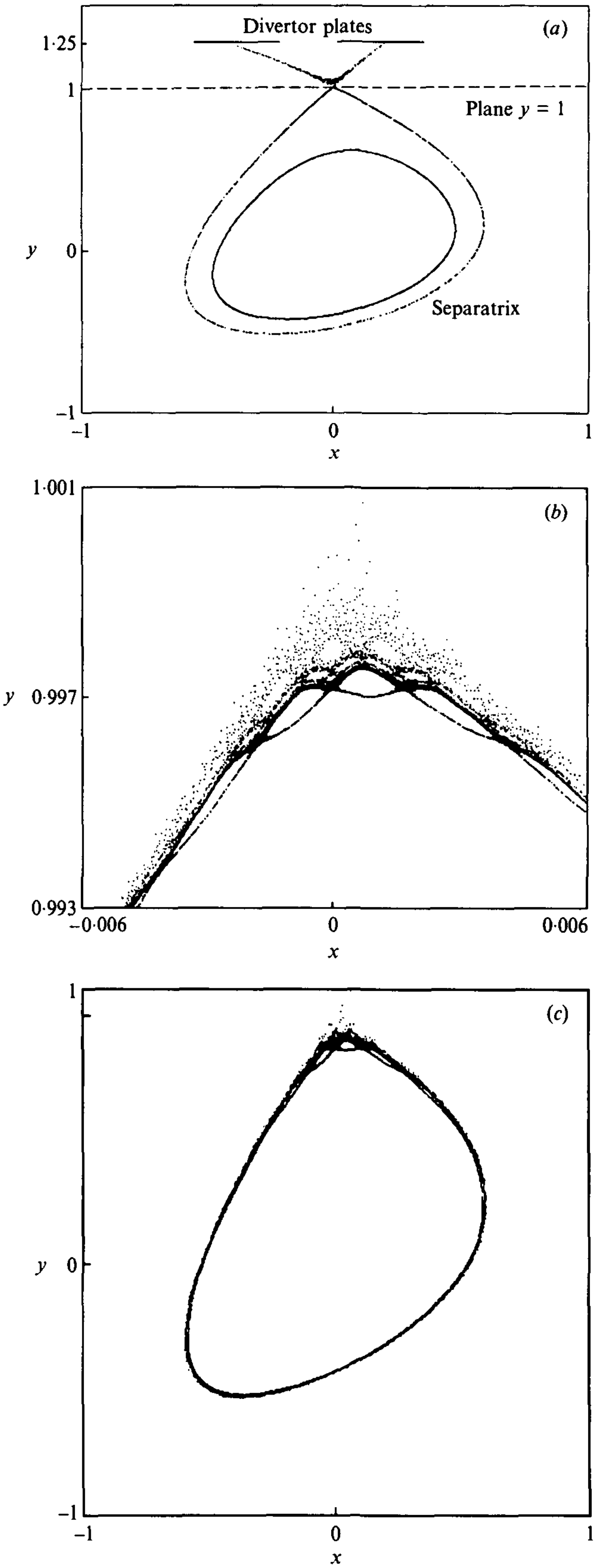

FIGURE 1. For caption see facing page.

of-freedom time-dependent Hamiltonian equations of motion. For our purpose, we want the maps and their continuous analogues to have toroidal geometry.

First, we present an example of such maps, called the simple tokamak divertor map.

4. Simple tokamak divertor map

The simplest divertor map has a single positive parameter k,

$$x_{n+1} = x_n - ky_n(1-y_n), \tag{1}$$

$$y_{n+1} = y_n + kx_{n+1}, \tag{2}$$

an O-point at $x = 0$, $y = 0$, and an X-point at $x = 0$, $y = 1$. The map provides a good representation of the magnetic field lines of a generic single-null tokamak divertor (figure 1*a*). Toroidal asymmetries can be simulated using k or by including additional terms. Here, toroidal asymmetries are simulated using k, but the results are not qualitatively changed by other representations. The smaller k is, the closer the last confining magnetic surface passes to the X-point. For $k = 0{\cdot}6$ the closest approach is $x = 0$, $y = 0{\cdot}997$ (figures 1*a*, *b*); for $k = 0{\cdot}9$ the closest approach is $x = 0$, $y = 0{\cdot}854$ (figure 1*c*). Each iteration of the map corresponds to a toroidal angular advance ζ_0. Near the O-point the rotational transform of the field lines per iteration, $\iota = 2\pi/q_1$, is

$$\sin(2\pi/q_1) = k(1-\tfrac{1}{4}k^2)^{\frac{1}{2}}. \tag{3}$$

One obtains a transform of roughly unity near the axis if 10 iterations of the map constitute a single toroidal circuit, $\zeta_0 = 2\pi/10$.

4.1. *Extensions of simple map*

The simple map can be extended to represent various magnetic features of divertor tokamaks. These include double-null divertors, realistic transform (e.g. high shear) and more physical perturbations, etc.

The magnetic topology of a double-null divertor tokamak can be adequately modelled by the map

$$x_1 = x_0 - ky_0(1-y_0)^2, \tag{4}$$

$$y_1 = y_0 + kx_1. \tag{5}$$

The rotational transform of divertor tokamaks can be reproduced if we consider $N_{\text{map}} \approx 10$ periods of the simple map to be equivalent to one toroidal circuit of a field line in a tokamak. To plot the intersection of trajectories with the divertor plates, we require the location of trajectories at arbitrary toroidal locations, not just at the principal planes of the discrete map. This can be accomplished by constructing the continuous analogue of the simple map.

FIGURE 1. (*a*) The simple map when the parameter $k = 0{\cdot}6$. The figure shows the separatrix, the plane $y = 1$ and the divertor plates. (*b*) Magnified view of the stochastic scrape-off layer near the X-point when $k = 0{\cdot}6$. This plot was done by iteration of the initial condition $x_0 = 0$, $y_0 = 0{\cdot}9971$. (*c*) Simple map when $k = 0{\cdot}9$. Now the last good surface passes near $x = 0$, $y = 0{\cdot}854$. The stochastic layer here is plotted from iterations with initial condition $x_0 = 0$, $y_0 = 0{\cdot}85492$.

Letting $\phi = \zeta/\zeta_0$, $0 \leqslant \phi \leqslant 1$, the (area-preserving) continuous analogue of the simple map is

$$x(\phi) = x_n - ky_n(1-y_n)\phi, \tag{6}$$

$$y(\phi) = y_n + kx(\phi)\phi. \tag{7}$$

Note that these equations are the solutions of Hamilton's equations of motion with

$$H(x,y) = -kx(x-x_0) - kyy_0(1-y_0), \tag{8}$$

where x is the canonical co-ordinate, y is the canonical momentum and ϕ is the canonical time. The continuous map is essential for finding the toroidal bunching of the location of field line strike points, as well for simplifying the Monte Carlo calculations for the heat-deposition pattern on the divertor plates.

Particles that have a negative parallel velocity follow the map backwards. The reverse of the simple map is

$$y_0 = y_1 - kx_1, \tag{9}$$

$$x_0 = x_1 + ky_0(1-y_0). \tag{10}$$

The simple map has low shear away from the separatrix. By adding terms to the simple map, the shear may be increased.

4.2. *Higher shear map*

An explicit map that has an adjustable shear s is

$$x_1 = x_0 - ky_0[(1-y_0)(1+sy_0)+sx_1^2], \tag{11}$$

$$y_1 = y_0 + kx_1[1+s(x_1^2+y_0^2)]. \tag{12}$$

Tokamak shear corresponds to negative s. For $k = \frac{1}{2}$ the ratio of ι at the X-point to ι at the surface that goes through $(x = 0, y = 0{\cdot}8)$ is 1·35 for $s = 0$ but 2·11 for $s = -0{\cdot}8$. Near the X-point at $(x = 0, y = 1)$ the map has the same form as the simple map, but with $k \rightarrow k(1+s)$. Thus it is possible to construct maps with variable shear.

4.3. *Perturbations*

The physical nature of tokamak perturbations that would give the stochasticity displayed by the simple map is unclear. However, we should like the perturbations to be more physical in their characteristics. This can be done by adding terms to the map that represent low-M, low-N perturbations as well as terms to that would represent a diffuser coil.

Low-M, low-N perturbations

Such perturbations arise naturally. An area-preserving map can be defined as

$$x_1 = x_0 - k\frac{\partial \Delta}{\partial y_0}, \quad y_1 = y_0 + k\frac{\partial \Delta}{\partial x_1},$$

with
$$\Delta = \Delta(x_1, y_0).$$

$\Delta(x,y)$ is called the generating function for the map. If $\Delta_0(x,y)$ is the unperturbed generating function then

$$\Delta(x,y) = \Delta_0 + \tfrac{1}{2}\delta(x^2-y^2)\cos\left(\frac{2\pi I}{N_p}\right), \tag{13}$$

with I the iteration number. This perturbation adds the effect of two quadrupoles with opposite helicity of toroidal mode number ±1.

High-M, high-N perturbations due to localized coils

The derivation by Martin & Taylor (1984) of the high-M and high-N perturbation due to localized coils gives

$$B_x = b\, e^{-\kappa y}\sin \kappa x, \tag{14}$$

$$B_y = b\, e^{-\kappa y}\cos \kappa y. \tag{15}$$

Here $\kappa = M/r$, where M is the poloidal mode number of the perturbation and r is the minor radius of the tokamak. These perturbed fields are practical only in the limit of high toroidal mode number N for a finite-aspect-ratio tokamak (Martin & Taylor 1984). Thus, by choosing sufficiently large κ, we can represent high-M, high-N perturbations.

The field lines are given by

$$\frac{dx}{dz} = \frac{B_x}{B_0}, \tag{16}$$

$$\frac{dy}{dz} = \frac{B_y}{B_0}. \tag{17}$$

Let
$$h(x,y) = \frac{b}{\kappa B}e^{-\kappa y}\sin \kappa x,$$

then
$$\frac{dx}{dz} = -\frac{\partial h}{\partial y} = \kappa h, \tag{18}$$

$$\frac{dy}{dz} = \frac{\partial h}{\partial y}. \tag{19}$$

Since h is independent of z, it is conserved. Now assume that the coil has a z length l that is very small compared with the tokamak circumference; then the jump in a field line is

$$x_1 = x_0 + \kappa l h(x_0,y_0) = x_0 + \delta\, e^{-\kappa y_0}\sin \kappa x_0, \tag{20}$$

with
$$\delta \equiv \frac{bl}{B_0}, \quad h(x_1,y_1) = h(x_0,y_0).$$

Therefore
$$y_1 = y_0 + \frac{1}{\kappa}\ln\left(\frac{\sin \kappa x_1}{\sin \kappa x_0}\right). \tag{21}$$

This map will be well behaved if $\kappa|x_1 - x_0| \ll 1$. We apply the diffuser map, (20) and (21), after each of the N_p iterations of the regular map required to represent the one full toroidal circuit of the tokamak if there is only a single diffuser coil.

4.4. *Deposition pattern of the field lines*

There are two ways in which we can study the deposition pattern of field lines on the divertor plates. In the first case we start the field lines just outside the last closed surface, where they undergo many circuits of the tokamak. In the second case we start the field lines inside the last closed surface, and radially diffuse them outwards after each iteration. We illustrate both methods when we discuss the application of the simple map.

5. General theory of maps

We have used maps to represent the features of magnetics of divertor tokamaks. Here we give a brief discussion of some relevant aspects of the general theory of maps.

Magnetic field lines are the trajectories of a single-degree-of-freedom Hamiltonian $H(x, y, \xi)$. An arbitrary trajectory $x = x(x_0, y_0, \xi)$, $y = y(x_0, y_0, \xi)$ is a Hamilton trajectory,

$$\frac{dx}{d\xi} = -\frac{\partial H}{\partial y}, \tag{22}$$

$$\frac{dy}{d\xi} = \frac{\partial H}{\partial x}, \tag{23}$$

if and only if it is area-preserving,

$$\frac{\partial(x, y)}{\partial(x_0, y_0)} = 1, \tag{24}$$

where the Jacobian

$$\frac{\partial(x, y)}{\partial(x_0, y_0)} \equiv \frac{\partial x}{\partial x_0}\frac{\partial y}{\partial y_0} - \frac{\partial x}{\partial y_0}\frac{\partial y}{\partial x_0}. \tag{25}$$

The trajectories change radically if the Hamiltonian structure (magnetic flux conservation) does not hold.

5.1. *Generating functions*

A map is area-preserving, $\partial(x_1, y_1)/\partial(x_0, y_0) = 1$, if and only if

$$x_1 = x_0 - k\frac{\partial \Delta_1}{\partial y_0} \tag{26}$$

and

$$y_1 = y_0 + k\frac{\partial \Delta_1}{\partial x_1}, \tag{27}$$

where $\Delta_1(x_1, y_0)$ is the generating function for the map. The connection between Hamiltonian mechanics and the topology of the map is determined by the map parameter k. In the limit of vanishing k, Δ_1 becomes the Hamiltonian. If Δ_1 is independent of iteration number, it is conserved by the map:

$$\Delta(x_1, y_1) = \Delta(x_0, y_0) + O(k^2). \tag{28}$$

For small k one can pick $\Delta(x, y)$ so that either the constant-Δ surfaces have the desired shape and/or the Hamiltonian $\Delta(x, y)$ has the desired shear.

5.2. *Explicit, reversed and continuous maps*

A map is explicit if the equation

$$x_1 = x_0 - k\frac{\partial\Delta(x_1, y_0)}{\partial y_0}$$

can be solved analytically, $x_1 = x_1(x_0, y_0)$. Implicit maps require more computation. The simple map is an example of the explicit map. It is possible to reverse any map:

$$y_0 = y_1 - k\frac{\partial\Delta(x_1, y_0)}{\partial x_1}, \tag{29}$$

$$x_0 = x_1 + k\frac{\partial\Delta}{\partial y_0}. \tag{30}$$

It is important to remember that for the backwards map to be explicit an analytical solution $y_0 = y_0(x_1, y_1)$ must exist. In our investigation we intend to use only explicit maps.

As mentioned earlier, we want to be able to determine the exact toroidal location of the field line or plasma particle. This requires a continuous analogue of the map. Any area-preserving map can be made continuous by letting

$$x(\xi) = x_0 - k\xi\frac{\partial\Delta}{\partial y_0}, \tag{31}$$

$$y(\xi) = y_0 + k\xi\frac{\partial\Delta}{\partial x}, \tag{32}$$

with $0 \leqslant \xi \leqslant 1$. The plane determined by the discrete map or $\xi = 0$ or 1 is called the principal plane. x_0 and y_0 must lie in the principal plane. Let $x(\xi) = x(x_0, y_0, \xi)$ and $y(\xi) = y(x_0, y_0, \xi)$; then $x_2 \equiv x(\xi_2) \neq x(x_1, y_1, \xi_2 - \xi_1)$. The continuous map is equivalent to a Hamiltonian that has a localized perturbation in each principal plane.

6. Monte Carlo calculations of the particle motion

Our aim is to determine the patterns of heat deposition on the divertor plates of a tokamak. To achieve this, we need to calculate the trajectories of the plasma particles in a divertor tokamak with a stochastic scrape-off layer. Plasma particles enter the stochastic scrape-off layer from the main plasma, where the magnetic surfaces are closed. Collisional effects cause the particles to diffuse across magnetic surfaces. The relevant kinetic equation is the Boltzmann equation with Lorentz collision operator:

$$\frac{\partial f}{\partial t} + v\frac{\partial f}{\partial l} = D\left(\frac{\partial^2 f}{\partial x^2} + \frac{\partial^2 f}{\partial y^2}\right) + C(f). \tag{33}$$

Here l is the distance along the magnetic field line, $C(f)$ is the collision operator, v is the velocity parallel to $\mathbf{B}$, D is the spatial diffusion coefficient, T is temperature, x and y are the rectangular co-ordinates in a plane normal to toroidal direction, and

$$C(f) = \frac{\partial}{\partial v}\left\{\nu\left[(v-u)f+\frac{T}{m}\frac{\partial f}{\partial v}\right]\right\} \tag{34}$$

is the collision operator. Here u is a flow velocity. Now the collision and diffusion operators can be represented by their Monte Carlo equivalents (Boozer & Petravic 1981; Punjabi *et al.* 1990). After a time step of length τ, the particle velocity is changed by collision from v_0 to v_1, with

$$v_1 = v_0-\nu\tau(v_0-u)\pm\left(\frac{2T}{m}\nu\tau\right)^{\frac{1}{2}}. \tag{35}$$

The position is changed by collisions from (x_0, y_0) to (x_1, y_1), with

$$x_1 = x_0\pm(D\tau)^{\frac{1}{2}}, \tag{36}$$

$$y_1 = y_0\pm(D\tau)^{\frac{1}{2}}. \tag{37}$$

The Monte Carlo procedure starts a particle with velocity v_0 in one of the principal planes of the map. After a time step τ, the particle has moved a distance $l = v_0\tau$, so the field line map is iterated l/L times, with $L = 2\pi R/N_p$ being the distance associated with one iteration. N_p is the number of iterations of the simple map that are equivalent to one circuit of the tokamak. The fractional part of an iteration is the ξ that was introduced to make the map continuous. The collision and diffusion Monte Carlo operators are applied, so one has the new values of x, y and v and one knows the fractional distance ξ. The particle located at (x, y, ξ) moves a distance $l = v\tau$ along the line in the next time step. We can use the backwards map to find the location of the field line in the previous Poincaré plane, and then iterate the map a distance $l/L+\xi$. Thus we can follow the particles from the plasma interior to the divertor plate. The electric sheath at the divertor plate implies that the electron with velocity v should be reversed at the plate unless $\frac{1}{2}mv^2 > e\phi_s$. The energy of the particle when it strikes the divertor plate can be calculated directly. To implement energy scattering as well as evolution of an arbitrary initial distribution function, the method developed by Boozer & Petravic (1981) and Punjabi and Boozer (see Punjabi *et al.* 1990) can be used.

7. An application of the simple map: stochastic broadening of the scrape-off layer

We have used the simple map to study stochastic broadening of the scrape-off layer in a single-null divertor tokamak. Stochastic broadening is calculated from the width of the footprint of particle trajectories on the divertor plates. We locate divertor plates in the plane $y = 1$. Plasma particles following the field lines are led into the stochastic region by diffusion, where they strike the divertor plate. The footprint on the divertor plate consists of one or more curved stripes (Punjabi *et al.* 1992). The width of the stripe on the divertor plates is uniquely determined by the stripe formed by field lines as they cross

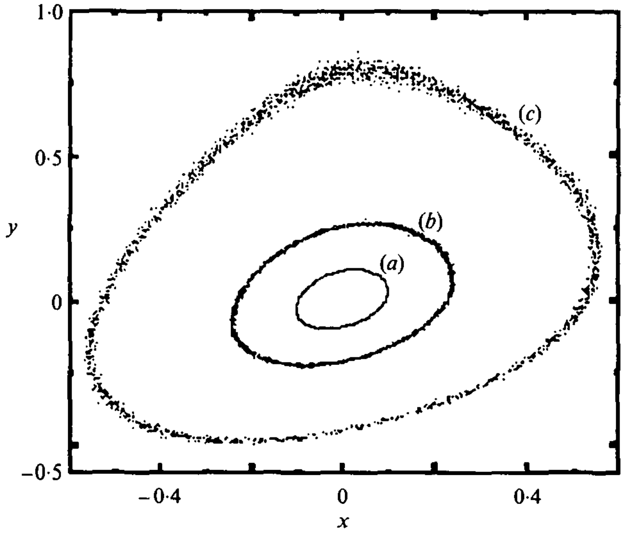

FIGURE 2. Application of radial expansion when $k = 0{\cdot}6$ and $\delta = 10^{-6}$. (*a*) represents 2048 trajectories passing through $x = 0$, $y = 0{\cdot}1$ in the principal plane. (*b*) and (*c*) represent (*a*) in the principal plane after $3{\cdot}5 \times 10^3$ and 7×10^3 applications of the radial expansion operator.

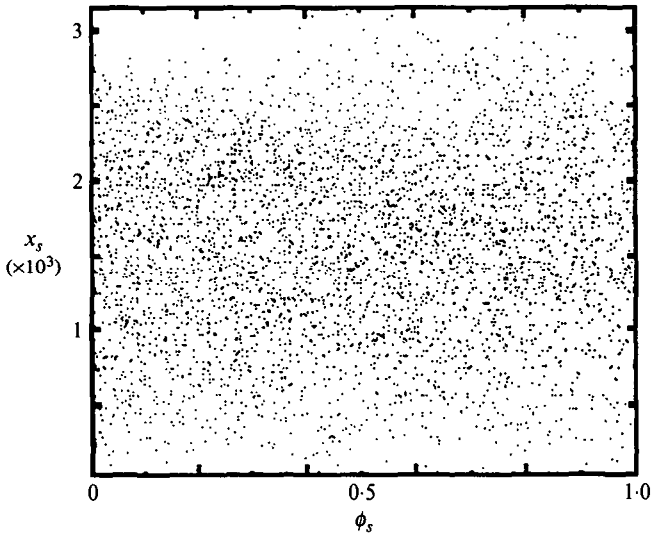

FIGURE 3. Footprint of trajetories on the divertor plate. Subscript *s* stands for 'strike'. (ϕ_s, x_s) are the ϕ and x co-ordinates of the strike points on the divertor plate. Trajectories start on the surface passing through $x = 0$, $y = 0{\cdot}5$, with $k = 0{\cdot}6$ and $\delta = 10^{-11}$. The footprint is a single stripe. The divertor plate is located in the plane $y = 1$.

the plane $y = 1$, which passes through the X-point. The toroidal location ζ at which field lines cross the (x, ζ) plane is determined using the continuous analogue of the discrete map, (6) and (7) above. The behaviour of field line trajectories that cross the last confining surface at a random point can be assessed by adding a small area-expanding step to each iteration of the discrete

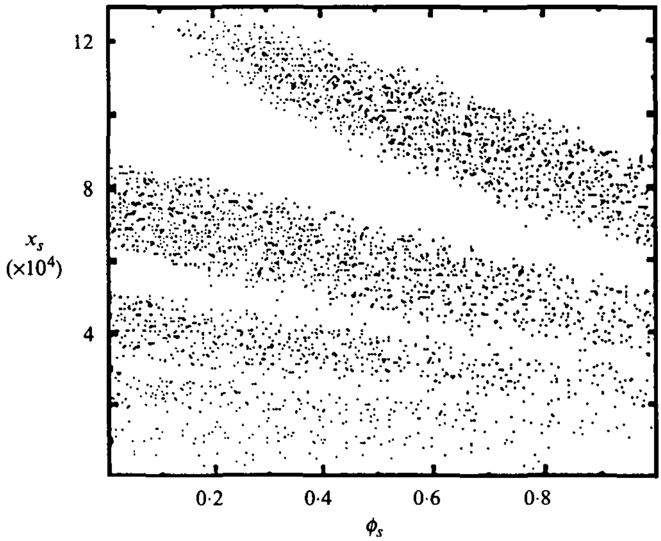

FIGURE 4. Footprint of trajectories starting on the surface going through $x = 0$, $y = 0{\cdot}5$ for $k = 0{\cdot}6$ and $\delta = 10^{-13}$. Now the footprint is made of helical stripes.

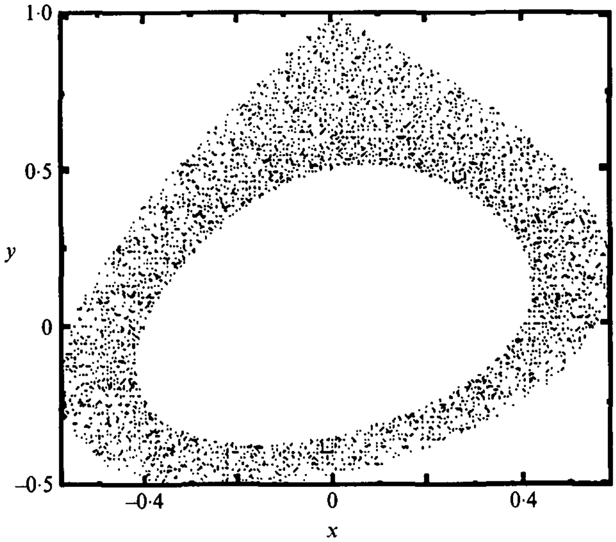

FIGURE 5. A typical Poincaré surface-of-section in the principal plane. The trajectory starts at $x = 0$, $y = 0{\cdot}5$, with $k = 0{\cdot}6$ and $\delta = 10^{-7}$. This figure represents 5×10^3 iterations.

map, $x_{\text{new}} = (1 + R\delta)\, x_{\text{old}}$, with R a random number between 0 and 1, and δ the expansion coefficient. For $k = 0{\cdot}6$ we find that for $\delta \ll 10^{-13}$ the strike points form helical stripes that are independent of δ. For larger values of δ the strike points form a single stripe, which has a width that scales as $\delta^{\frac{1}{4}}$. From the physical point of view, we want this stripe to have as large an area as possible, so that the heat flux density is a minimum. This means that we should like the magnetic flux from the stochastic scrape-off layer striking the divertor plates to be as large as possible.

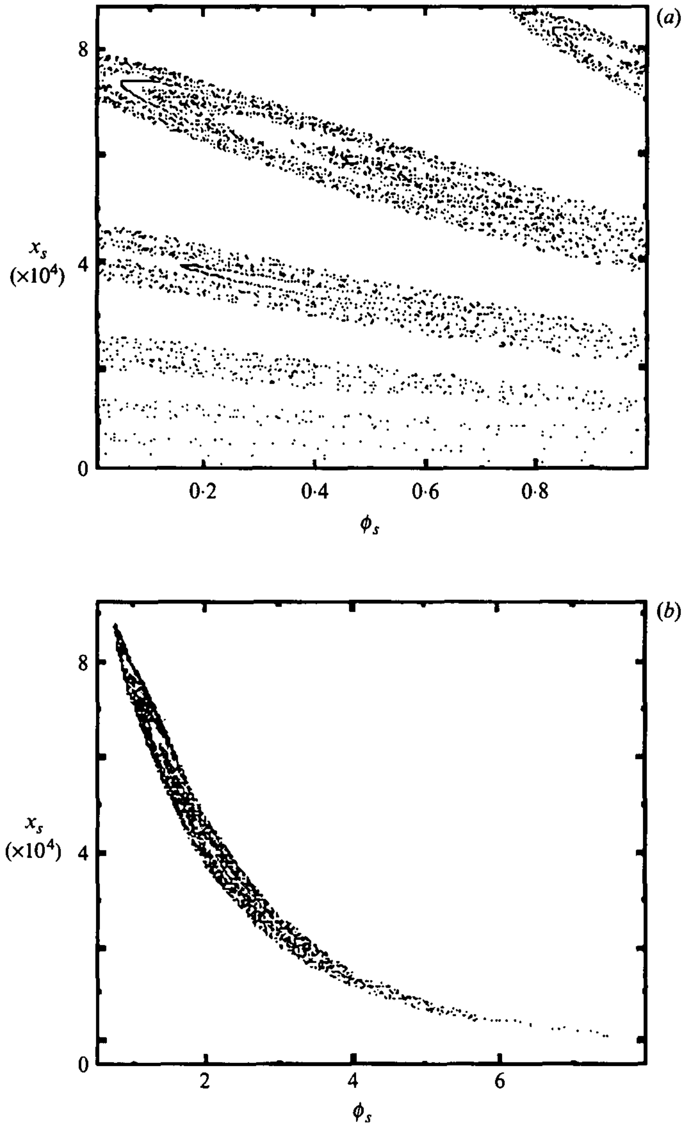

FIGURE 6. (*a*) Footprint of the strike points on the divertor plate when $\delta = 0$. The trajectories start in the scrape-off layer at $x_0 = 0$ and $0{\cdot}977 < y_0 < 1$. (*b*) When the footprint for $\delta = 0$ is unfolded in the ϕ direction, we get a sharp, narrow helical stripe.

7.1. *Stochastic broadening*

To simulate plasma-particle trajectories in a single-null divertor tokamak, we start with 2048 particles on the flux surface passing through $(x = 0, y = \frac{1}{2})$. The trajectories of these particles are evolved using the Hamiltonian equations. At the end of each toroidal circuit, the radial expansion operator is applied. Figure 2 shows the application of the radial expansion operator. The (x, ϕ) co-ordinates of the intersections of trajectories with the plate are recorded until half of the particles have struck the plate. This gives the footprint of the stochastic layer on the plate. The width of this footprint is defined as the standard deviation in

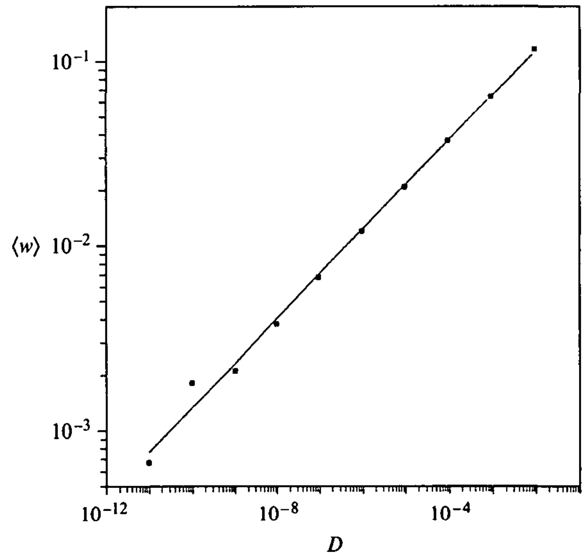

FIGURE 7. Scaling of average width $\langle w \rangle$ with radial expansion coefficient δ. The error in the mean is less than 1%.

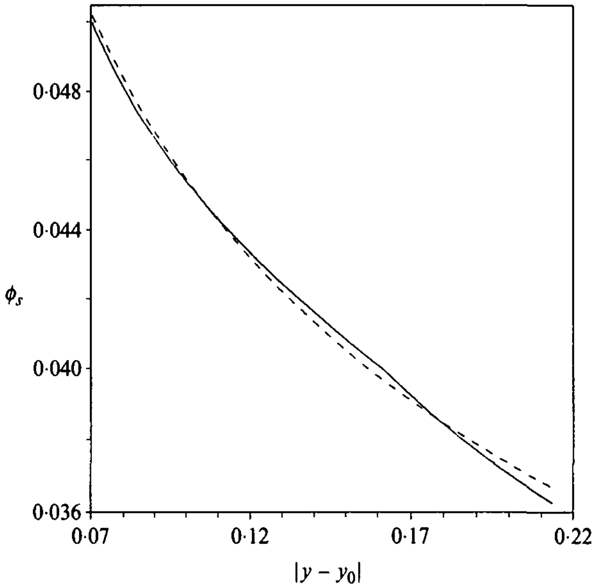

FIGURE 8. Plot of ϕ_s as a function of $\Delta y = |y - y_0|$. The trajectories start just outside the last good surface through $x = 0$, on the far side of the X-point. Here $k = 0{\cdot}6$ and $\delta = 0$. The solid line represents the ϕ co-ordinate of the strike point, ϕ_s, as a function of Δy. The dashed line is the fit $\phi_s = 0{\cdot}24\Delta^{-0{\cdot}28}$.

the x co-ordinate of the strike points. Stochastic broadening is the width in the limit of vanishing δ. We find that when $\delta > 10^{-13}$, the footprint is a single stripe. For $\delta \lesssim 10^{-13}$, the strike points form helical stripes. Figure 3 shows the single stripe, and figure 4 shows helical stripes. Figure 5 shows a typical Poincaré

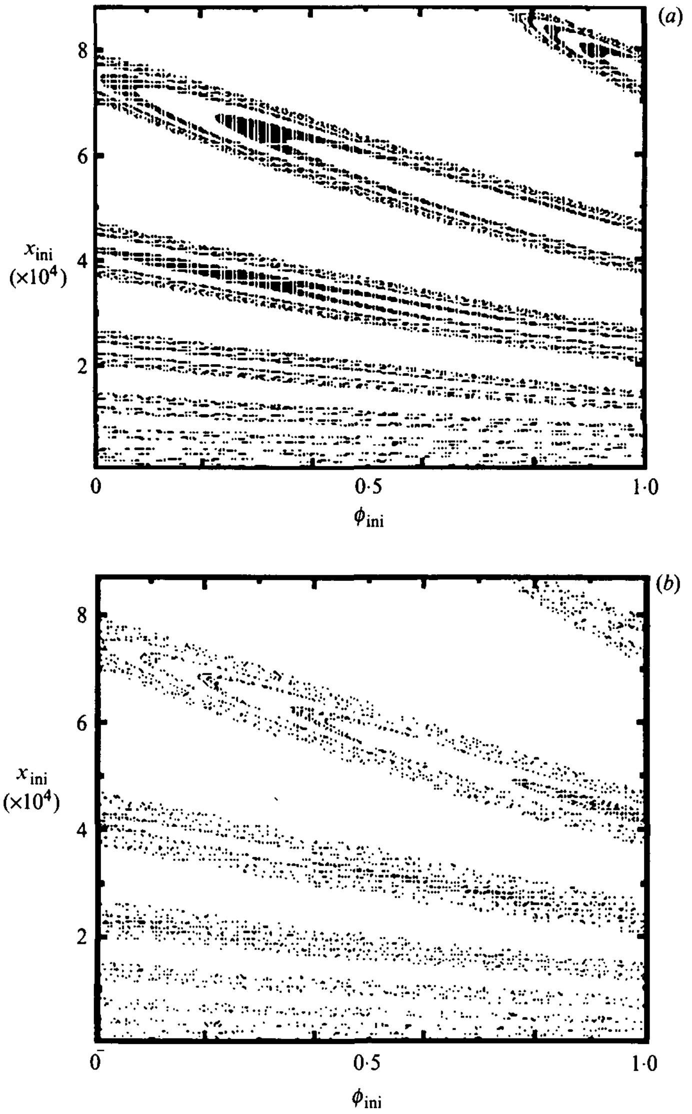

FIGURE 9. (*a*) The points in the helical strip corresponding to numbers of poloidal circuits, N_p, between 1 and 2 exhibit a concentric ring-like structure. We reverse-integrate a very large number of trajectories, starting on the divertor plate on the positive-x side. The trajectories start on uniformly distributed grid points in a rectangle exactly accommodating the helical stripe. This plot shows the grid points whose reverse trajectories strike the divertor plate on the negative-x side with $1 \leqslant N_p < 2$. (*b*) Grid points whose reverse trajectories strike the other side of the plate with $2 \leqslant N_p < 3$.

surface-of-section for one trajectory. To obtain the footprint in the limit as $\delta \rightarrow 0$, we put $\delta = 0$ and start trajectories in the scrape-off layer near the X-point. When unfolded in the ϕ direction, the footprint is a narrow and sharp helical stripe (figure 6). For the single-stripe case the average width of the footprint varies as $\delta^{\frac{1}{4}}$:

$$\langle w \rangle \propto \delta^{\frac{1}{4}}. \tag{38}$$

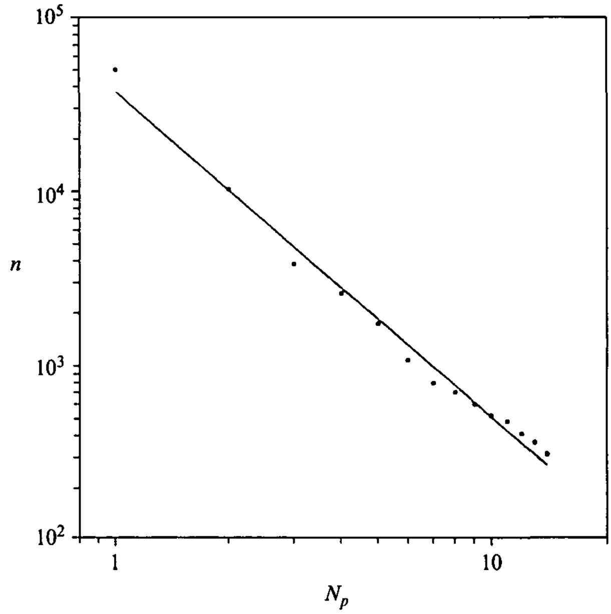

FIGURE 10. Graph of n versus N_p. We integrate a very large number of trajectories backwards. They start on the divertor plate on the positive-x side on uniformly distributed grid points in a rectangle that exactly accommodates the helical stripe. Solid squares represent n as a function of N_p, where n is the number of trajectories that strike the other side of the plate after a fixed number N_p of poloidal transits. The solid line is the fit, $n = 37\,227 N_p^{-1.89}$.

This is shown in figure 7. For $\delta \ll 10^{-13}$ the average width is independent of δ. The $\delta^{\frac{1}{4}}$ scaling is the result of the scaling $\Delta y \propto \phi^{-\frac{1}{4}}$ (figure 8). Field lines in the stochastic layer spend the majority of time in the proximity of the X-point.

We generate a rectangular mesh on one side of the divertor plate. We consider the nodes of this mesh as the strike points of trajectories on the divertor plate. Now we use the backward map, (9) and (10), and its continuous analogue to calculate the starting points of these trajectories on the other side of the divertor plate. We also record the number of poloidal circuits it takes each trajectory to traverse from one side of the divertor plate to the other. From this exercise, we observe a number of interesting features. The helical stripe is actually the footprint of the trajectories that circle the magnetic axis at least once. Within this stripe, the points corresponding to different values of poloidal transits show concentric rings. We denote the number of poloidal transits by N_p. In figure 9 we show the rings corresponding to $N_p = 2$ and 3. In figure 10 we plot the number n of open field lines, for a given fixed number N_p of poloidal transits. From this plot, we see that

$$n \propto N_p^{-2}. \qquad (39)$$

From this, we conclude that the area of the helical stripe varies as the inverse square of the number of poloidal transits for the open field lines.

In figures 11–13 we present some data on the distribution of strike points within the helical stripe. In the x direction the distribution is skewed towards the

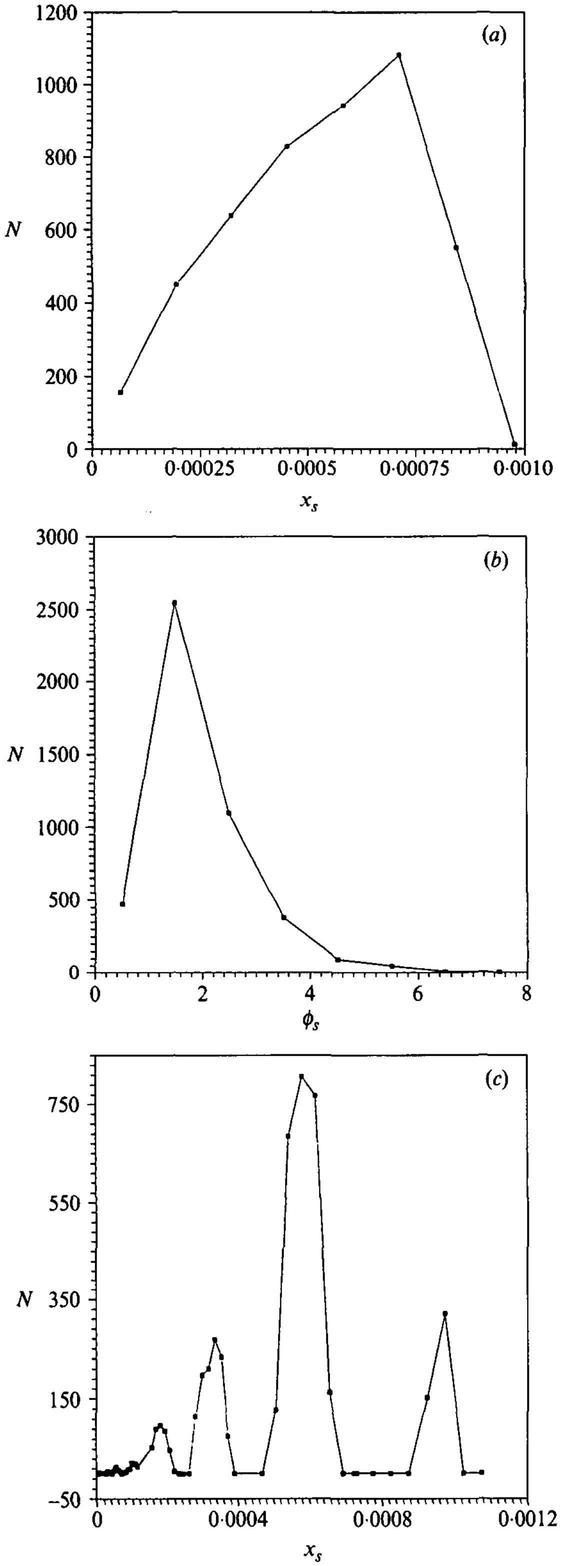

FIGURE 11. (*a*) Distributions of strike points in the helical stripe: (*a*) in the x direction; (*b*) in the ϕ direction; (*c*) transverse to the stripe.

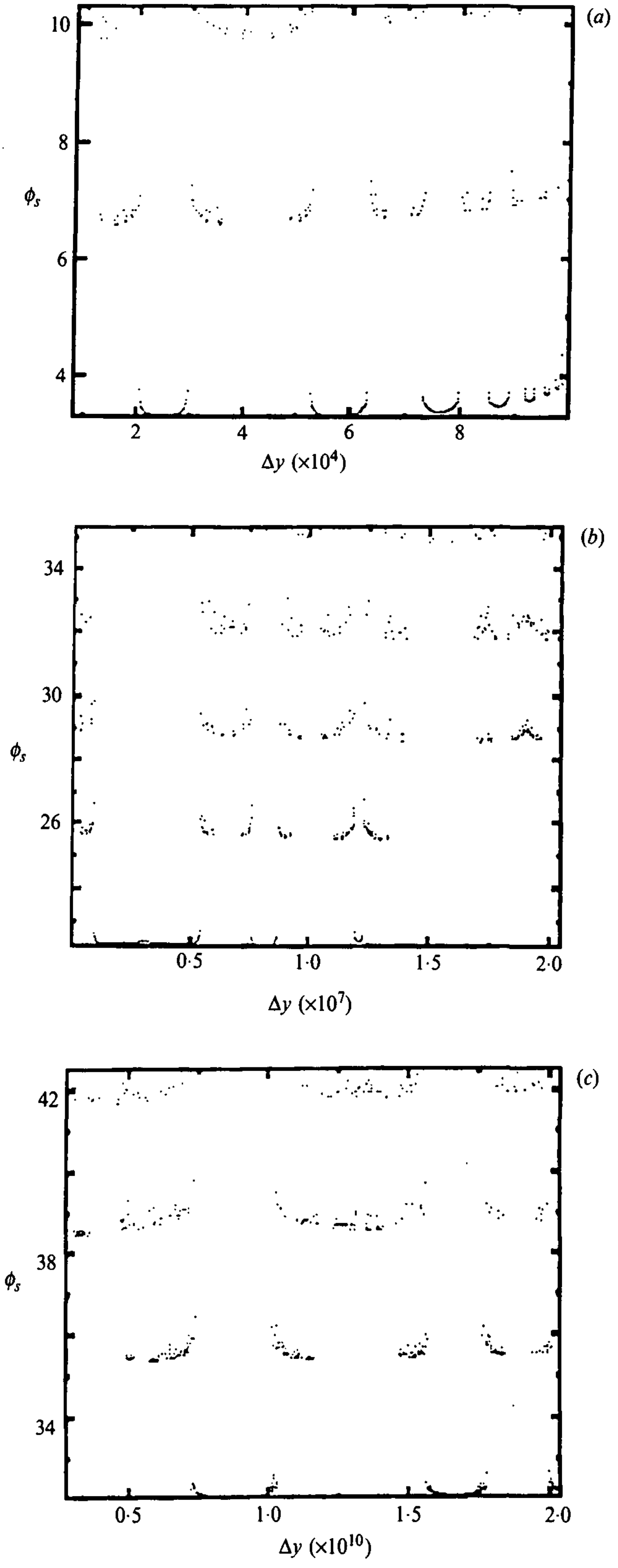

FIGURE 12. For caption see facing page.

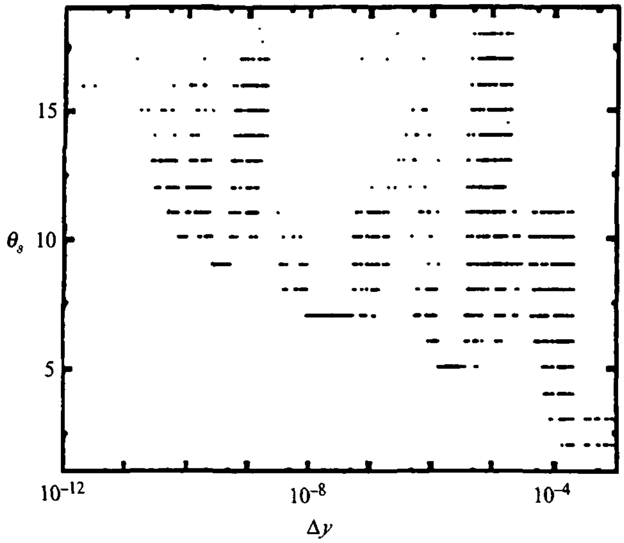

FIGURE 13. Dwelling time in the poloidal direction θ_s as a function of Δy.

X-point (figure 11*a*). In the ϕ direction the distribution is skewed towards increasing ϕ (figure 11*b*). Transverse to the stripe, the distribution is normal (figure 11*c*). We also observe that the dwelling time in the toroidal direction for the open field lines before they strike the divertor plate has a self-similar pattern as shown in figure 12, while the dwelling time in the poloidal direction has a discrete structure as shown in figure 13.

7.2. *Summary of results*

Particles that diffuse across the last confining surface of a tokamak with a divertor can follow open magnetic field lines to the divertor plates. The strike points of these field lines on the divertor plates lie in discrete stripes. The region between the last confining magnetic surface and the separatrix of the ideal divertor is called the stochastic layer. The open magnetic field lines of the stochastic layer enter the region from one divertor plate and leave, striking another divertor plate, after an integer number N_p of complete poloidal circuits. The discrete stripes on the divertor plates correspond to the number of poloidal circuits made by open field lines. The area of the stripes scales as N_p^{-2}. The open field lines that approach the last confining surface make many poloidal circuits before striking a divertor plate in a stripe that is much narrower than the stochastic layer ($\approx 15\%$) but none the less of non-zero width. An open field line that makes many poloidal circuits in going from one divertor plate to another in essence densely fills the stochastic layer except for the regions in the latter that are occupied by magnetic islands.

FIGURE 12. Dwelling time for trajectories in the toroidal direction ϕ_s as a function of distance $\Delta y = |y - y_0|$ from the last good surface. The trajectories start on the line $x = 0$ in the scrape-off layer. We determine the number of toroidal circuits. N_s, that it takes the trajectories to reach the divertor plate as a function of distance Δy. (*a*) $\Delta y = 10^{-4}$; (*b*) 10^{-7}; (*c*) 10^{-10}.

7.3. *Discussion of results*

In an axisymmetric divertor the spreading of the heat is due to plasma transport, which is often modelled by a diffusion coefficient D of order 1 $\mathrm{m}^2\,\mathrm{s}^{-1}$. During the time τ that the plasma takes to flow to the divertor chamber, the plasma diffuses across open magnetic field lines that contain a flux proportional to $(D\tau)^{\frac{1}{2}}$. The open field lines that contain flowing plasma have the same magnetic flux near the main body of the plasma and near the divertor plates.

By adding asymmetric magnetic perturbations, one can widen the region of heat deposition on the divertor plates. However, we find that the magnetic flux of the open field lines in the stochastic region is a factor of roughly six larger than the width in flux of these field lines when they strike the divertor plate. In effect, the open field lines of the stochastic region encircle the plasma roughly six times before striking the divertor plates. The relatively thick region of plasma flowing along open field lines in the stochastic region may provide an important shielding of the main plasma from impurities.

Magnetic field line trajectories are the trajectories of a $1\frac{1}{2}$-degree-of-freedom Hamiltonian (Boozer & Rechester 1978; Cary & Littlejohn 1983). Consequently, the tokamak separatrix and divertor are archetypal for the behaviour of a region of bounded Hamiltonian trajectories surrounded by a region of open trajectories. Plasmas flow rapidly along magnetic field lines and diffuse slowly across them. The study of magnetic field line behaviour and the closely related plasma behaviour are important not only for their application to tokamaks but also for their application to other Hamiltonian, or near-Hamiltonian, systems.

The behaviour of field lines near a tokamak separatrix has been studied previously. Early work (Boozer & Rechester 1978) used the Chirikov island overlap criterion, which is a reasonable approximation for calculating the stochastic region but overestimates the spreading of heat on the divertor plates. Recently, Pomphrey & Reiman (1992) integrated magnetic trajectories in a field produced by wires. They noted that the extremely thin spiral regions of impact of magnetic field lines started near the last closed surface on the divertor plates.

The major advantage of our method is that field line trajectories can be followed many orders of magnitude faster with a map than with an explicit integration. The speed of map iterations allows one to study the structures formed by the perturbations in more detail and to investigate the effects of qualitatively different types of perturbations.

The complicated filling of the stochastic region by the open field lines gives an associated complexity to the ambipolar electric potential that exists along any open magnetic field line that is embedded in a plasma. Although we have not calculated the particle transport from the $\mathbf{E}\times\mathbf{B}$ drifts associated with the ambipolar potential, we expect a diffusive effect that would smear the stripe structures.

This work is supported by United States Department of Energy Grants DE-FG05-88ER53265 and DE-FG05-90ER54106.

REFERENCES

Boozer, A. 1983 *Phys. Fluids* **26**, 1288.

Boozer, A. & Petravic, G. 1981 *Phys. Fluids* **24**, 851.

Boozer, A. & Rechester, A. 1978 *Phys. Fluids* **21**, 682.

Cary, J. R. & Littlejohn, R. G. 1983 *Ann. Phys. (NY)* **151**, 1.

Le Haye, R. J. 1991 *Nucl. Fusion* **31**, 1550.

Lichtenberg, A. J. & Liberman, M. A. 1983 *Regular and Stochastic Motion.* Springer.

Martin, T. J. & Taylor, J. B. 1984 *Plasma Phys. Contr. Fusion* **28**, 321.

Pomphrey, N. & Reiman, A. 1992 *Phys. Fluids* B **4**, 938.

Post, D. E. *et XXXVII al.* (and other International contributors) 1991 *ITER Physics. ITER Documentation Series* no. 21. IAEA.

Punjabi, A., Boozer, A., Lam, M., Kim, M. & Burke, K. 1990 *J. Plasma Phys.* **44**, 405.

Punjabi, A., Verma, A. & Boozer, A. 1992 *Phys. Rev. Lett.* **69**, 3322.

Whittaker, E. T. 1937 *A Treatise on the Analytical Dynamics of Particles and Rigid Bodies.* Cambridge University Press.